

Delta Power Control Strategy MPPT & CPG for Multistring Grid-Connected PV Inverters

Lavudya Jayasree¹
Gairaboina Nagaraju²

ASSISTANT PROFESSORS

CHRISTU JYOTHI INSTITUTE OF TECHNOLOGY & SCIENCE
COLOMBO NAGAR, YASHWANTHAPUR, JANGOAN T.S

Abstract—With a still increasing penetration level of grid-connected photovoltaic (PV) systems, more advanced active power control functionalities have been introduced in certain grid regulations. A delta power constraint, where a portion of the active power from the PV panels is reserved during operation, is required for grid support (e.g., during frequency deviation). In this paper, a cost-effective solution to realize delta power control (DPC) for grid-connected PV systems is presented, where the multistring PV inverter configuration is adopted. This control strategy is a combination of maximum power point tracking (MPPT) and constant power generation (CPG) modes. In this control scheme, one PV string operating in the MPPT mode estimates the available power, whereas the other PV strings regulate the total PV power by the CPG control strategy in such a way that the delta power constraint for the entire PV system is achieved. Simulations and experiments have been performed on a 3-kW single-phase grid-connected PV system. The results have confirmed the effectiveness of the proposed DPC strategy, where the power reserve according to the delta power constraint is achieved under several operating conditions.

Index Terms—Active power control, constant power generation (CPG) control, grid-connected power converters, maximum power point tracking (MPPT), power reserve control, photovoltaic (PV) systems.

I. INTRODUCTION

PHOTOVOLTAIC (PV) systems have been increasingly in-

tegrated into the power grid in recent years, mainly driven by the continuous reduction in the price of PV panels as well as the system installation costs [1]–[3]. More PV systems are expected to be installed in the future and will share a major part of the power production, especially in residential-scale

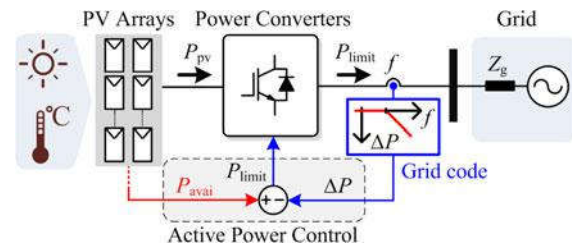


Fig. 1. Grid-connected PV systems with frequency-dependent active power reduction control, where P_{pv} is the PV output power, P_{limit} is the power limit level (injected output power), P_{avai} is the available PV output power, P is the required amount of power reserve, and f is the grid frequency.

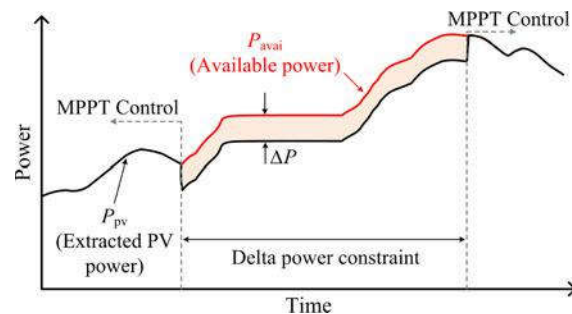


Fig. 2. Delta power constraint defined in the Danish grid code, where P is the amount of power reserve level [6].

systems [3]. Accordingly, the importance of PV participation in the grid control becomes clear, and is being introduced in certain grid regulations [4]–[8]. For instance, in Germany, the frequency-dependent active power reduction has been introduced for medium-voltage systems, as shown in Fig. 1 [4]. Similar requirements have also been defined in other grid codes [5], [6], where PV systems are not allowed to be immediately disconnected from the grid in the case of frequency deviations. Instead, the output active power from the PV systems has to be reduced to a certain level, in order to support the grid and also to provide power reserve. In the Danish grid code, a delta power constraint is defined [6] (also called power reserve control), whose operational principle is illustrated in Fig. 2. Notably, the delta power constraint is currently used for potential frequency responses in large-scale PV power plants. As the penetration level of grid-connected PV systems is still increasing, this requirement is also expected to be introduced in small and medium-scale PV power plant. In those cases, a majority of PV systems are (and will continue to be in the future) adopted in residential/commercial applications [3].

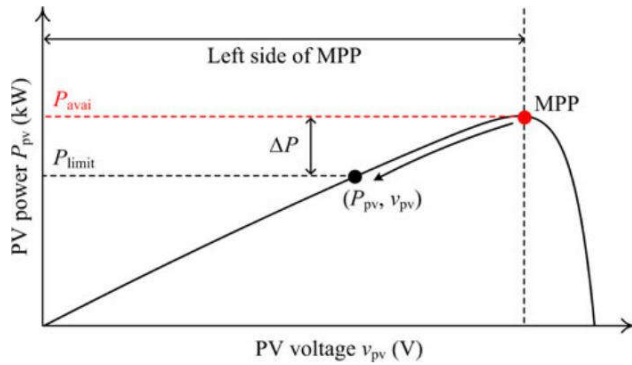


Fig. 3. P-V characteristic of the PV panels with the operating point at the power limit P_{limit} , where maximum power point.

When looking into the prior artwork, there are mainly three approaches to realize delta power control (DPC) [8]–[11]: integrating energy storage systems, applying a dump load to dissipate excessive power, and limiting the extracted PV power by modifying maximum power point tracking (MPPT) algorithms. Integrating energy storage systems is one of the most commonly used solution, where the surplus PV power can be stored in the energy storage device (e.g., batteries), and thus the PV power can be reserved during operation. One key benefit of this solution is that it can also provide an upward frequency regulation, meaning that the PV system can inject power higher than the maximum available power by discharging the energy storage device. This is beneficial for grid support especially during the low PV power production periods (e.g., at night). However, high cost and limited lifetime are usually associated with this approach, making it not very feasible. This can challenge the overall cost of PV energy, which is against the high expectation of cost reduction in the next decade [12]. Another solution to the power reserve is by installing a dump load to dissipate the surplus PV power. However, this solution also requires extra components (e.g., resistance load with a controller to regulate the power flow), thus increasing the overall system complexity [13], [14]. Therefore, the third approach by modifying the MPPT algorithm offers a more cost-effective solution, and will be considered in this paper.

In this approach, the operating point of the PV system in the power-voltage (P-V) curve is regulated below the maximum power point (MPP) in order to limit the PV power P_{pv} to a certain level P_{limit} , as shown in Fig. 3. Operating the PV system below the MPP is not a new issue, as it has been previously applied to other applications (e.g., constant power generation (CPG), microgrid, fault-ride through) [15]–[27]. However, the challenge to realize the DPC strategy is the estimation of the available PV output power P_{avai} during operation, which is required in order to calculate the setpoint P_{limit} according to the delta power constraint (i.e., $P_{limit} = P_{avai} - P$) [9], [10], [27], [28]. One method to estimate the available PV power is to use the irradiance measurement, together with the PV array characteristic model, as suggested in [9], [11]. However, this method requires an accurate irradiance measurement, which is usually not available in the residential-scale PV systems (e.g., roof-top applications) considering the cost. In addition, a highly accurate

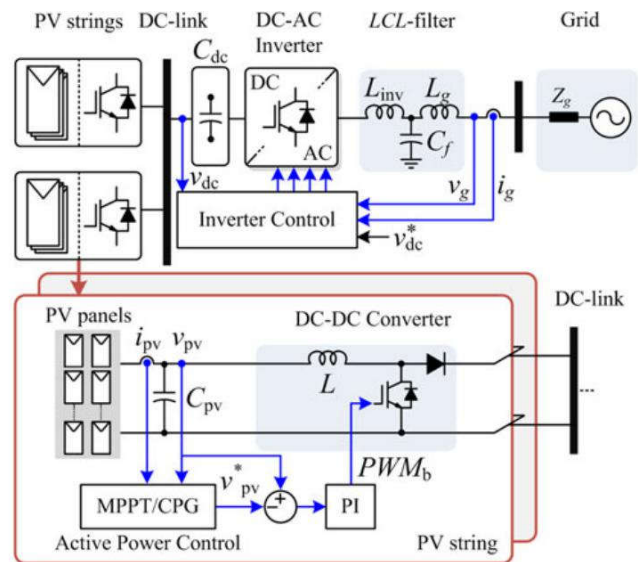


Fig. 4. System configuration and control structure of multistring grid-connected PV inverters [29].

model of the PV arrays is needed, which is typically not feasible due to aging, faults, etc. This will increase the cost and the complexity of the overall system. Alternatively, the available power P_{avai} can be estimated by means of a quadratic approximation curve-fitting method [10], [28], where the irradiance measurement is not required. In this approach, the PV voltage at the MPP V_{MPP} is first estimated from the present operating condition. Then, the estimation of the PV power at the MPP is achieved by using the estimated V_{MPP} with a combination of linear and quadratic approximation [28]. However, this method also relies on a model-based approach, which is not very generic and the estimation accuracy is compromised (due to the curve-fitting approximation). In light of the above discussions, it calls for a simple but effective solution to estimate the available PV power P_{avai} and thus to flexibly regulate the extracted PV power P_{pv} according to the delta power constraint.

Actually, most residential/commercial PV systems (e.g., with the rated power of 1–30 kW) usually employ a multistring PV inverter topology [29]–[33], whose system configuration is shown in Fig. 4. Recently, this string inverter topology is also becoming more and more popular in large-scale PV power plants, where a traditional central inverter is replaced by several string/multistring PV inverters, due to reduced installation cost, maintenance cost, and increased reliability [34], [35]. In this system configuration, the PV power extraction of each PV string is independently controlled by a dc-dc converter (e.g., a boost converter) equipped at each PV string. Normally, the MPPT algorithm is employed for each dc-dc converter, in order to maximize the PV energy yield. However, it is also possible to coordinately control several PV strings with different active power control strategies, in order to realize a power reserve control (i.e., the DPC strategy) [36]. In particular, one (or more) master PV string is assigned to operate in the MPPT mode and estimate the available PV power P_{avai} , whereas the other PV strings are controlled as slave systems to operate in the

CPG mode (also called active power reserve in some literature), where the power limits P_{limit} are set according to the master PV string. In this way, the total PV power production can be flexibly controlled considering the delta power constraint. This approach requires neither energy storage systems nor irradiance measurements, and it is being a cost-effective solution. This concept has been briefly discussed in [23], [37], [38]. However, a detailed explanation of the coordinated control algorithm to realize the DPC strategy in multistring PV systems has not yet been discussed in the literature. That is to say, there is still a gap between the conceptual discussion and the practical implementation of the DPC strategy. In addition, performance verification of the DPC strategy in real operation has not been investigated (e.g., during different solar irradiance conditions).

The main aim of this paper is to present the DPC control scheme applied to the multistring PV system. The detailed explanation of the coordinated control between the master PV string (with MPPT mode) and the slave PV strings (with CPG mode) is given in § III. This includes the discussion about the concept of the DPC strategy as well as the control algorithm for implementation. Then, simulations and experiments on a 3-kW two-stage PV system are conducted in § IV to verify the effectiveness of the DPC strategy under several test conditions. Finally, concluding remarks are given in § V.

II. SYSTEM CONFIGURATION AND CONTROL SCHEME OF MULTISTRING PV INVERTERS

In grid-connected PV applications, several system configurations can be adopted depending on the power rating of the PV power plant [29]–[31]. In residential-/commercial-scale PV systems (e.g., rated power of 1–30 kW), a two-stage conversion system, consisting of a dc–dc and a dc–ac conversion stages, is normally required. This is usually referred to as a multistring inverter configuration shown in Fig. 4, and it has been widely adopted commercially in this power range [32], [33]. In the first dc–dc conversion stage, each PV string, consisting of several PV panels connected in series and/or parallel, is equipped with a dc–dc boost converter to step up the PV voltage v_{pv} to match the required dc-link voltage v_{dc} . This is due to the fact that the PV voltage from the PV arrays in residential-/commercial-scale PV systems can vary in a wide range. In some cases, it may be lower than the minimum level of the dc-link voltage (e.g., 450 V) for grid-connected PV inverter, due to a limited number of PV panels connected in series.

Typically, the boost converter also performs the active power control (e.g., the MPPT control or the CPG control) for each PV string individually. This gives a possibility to coordinate the active power control of each PV string in order to achieve the delta power constraint. This will be discussed in the next section. The total extracted power by the dc–dc converters is subsequently delivered to the dc-link. Then, one dc–ac inverter is employed in the dc–ac conversion stage to inject the extracted PV power to the ac grid. This is normally achieved by regulating the dc-link voltage to be constant through the control of the grid current i_g [39]. As the PV power extraction is mainly controlled by the boost

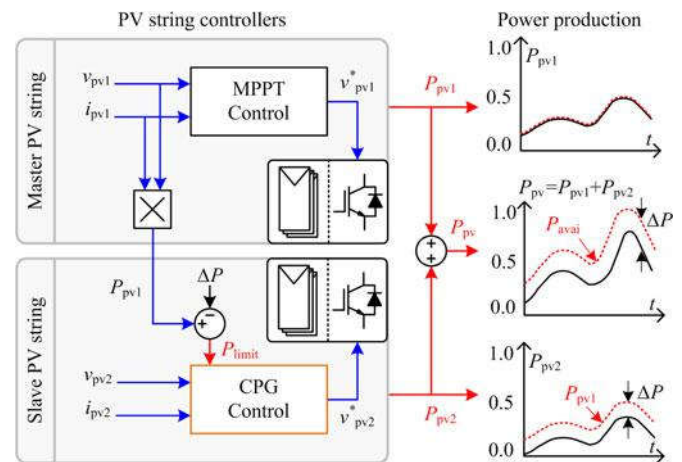


Fig. 5. Control scheme of the DPC strategy and the resultant power production, where the master and slave PV strings operate in the MPPT and the CPG modes, respectively.

dc–dc converter, the control algorithm in the dc–dc conversion stage to realize the DPC strategy is the main focus of this paper. Notably, the discussed control scheme can be generally applied to any two-stage PV system configuration, e.g., with different inverter hardware topologies, as they share the same overall control scheme.

III. DPC STRATEGY FOR MULTISTRING PV INVERTERS

The PV system needs to reserve a certain amount of PV power P during operation for possible frequency regulation, where the delta power constraint can be summarized as

$$P_{\text{pv}} = P_{\text{avai}} - P. \quad (1)$$

In order to control the PV output power P_{pv} according to the DPC strategy in (1), the other two quantities (i.e., the available power P_{avai} and the amount of power reserve P) must be known. Typically, the amount of power reserve P can either be calculated as a function of the grid frequency deviation or set by the system operator [9]–[11]. Thus, two challenging issues remain: 1) estimating the available power P_{avai} during the operation without irradiance measurements and 2) regulating the extracted PV power P_{pv} according to the DPC constraint in (1). As mentioned previously, the available power can be estimated by one of the PV strings that performs the MPPT control, whereas the latter issue can be achieved by the CPG control strategy [17]. Thus, the focus of this paper is on the active power control of the PV string (see Fig. 4), where the MPPT and the CPG operation are coordinately controlled. For the sake of simplicity, two PV strings with equal rated power in Fig. 4 are considered. The control structure is further illustrated in Fig. 5 and the total output power can thus be expressed as

$$P_{\text{pv}} = P_{\text{pv1}} + P_{\text{pv2}}. \quad (2)$$

A. Estimation of the Available Output Power—MPPT Operation for the Master PV String

Estimating the available PV power is very challenging, especially when the solar irradiance is not measured. However, PV strings in residential-/commercial-scale PV systems are usually located close to each other (e.g., on the same rooftop), in order to maximize the space utilization. This implies that most PV strings will have similar solar irradiance and ambient temperature profiles, and therefore similar power production profile. If one PV string as the master operates in the MPPT mode, its output power P_{pv1} can be used to estimate the available power of the rest PV strings as the slaves. Thus, the total available power of the PV plant P_{avai} can be simply estimated by multiplying P_{pv1} with the number of PV strings as

$$P_{avai} \approx N_{pv} P_{pv1} \quad (3)$$

where N_{pv} is the ratio between the rated power of the total PV plant and the rated power of the master PV string. For instance, if the PV system consists of two PV strings (i.e., one master string and one slave string) with the equal rated power (e.g., same total number of PV panels) considered in this paper and illustrated in Fig. 5, the power ratio can be determined as $N_{pv} = 2$. That is, the rated power of the master PV string is a half of the total PV system rated power.

By doing so, the total available power of the PV plant can be estimated without the solar irradiance measurement nor an accurate PV panel characteristic model, being a cost-effective solution. It is worth mentioning that this is based on the assumption that the mismatch between each PV string (e.g., due to faults, aging, partial shading) is very small.

Notably, in the case of a larger scale PV plant (i.e., more PV strings), several PV strings can be assigned to perform the MPPT operation (as master PV strings). Then, there are two possibilities for estimating the available power of the PV plant: 1) Global estimation—the averaged value of output power from all master PV strings is used globally for estimating the available power of the total system or 2) local estimation—the measured output power of each master PV string is used locally for estimating the available power of a local group of PV strings. The choice between the two approaches is not obvious as it depends on both the physical arrangement and the economic factor of the systems. The global estimation offers a simple implementation but the accuracy is compromised, especially for a large area PV plant, where the solar irradiance profile of different PV strings can vary considerably. Thus, it is not very suitable for a large-scale PV system with a wide-area distribution. On the other hand, the local estimation offers a higher estimation accuracy, but all the local groups of PV strings need to be coordinately controlled by a central controller in order to ensure that the total output power follows the DPC constraint in (1). This leads to more complicated control algorithms and costly communication systems, which may not be suitable for a small-/medium-scale PV plant. Moreover, the maximum power reserve level also decreases with the increased number of master PV strings (as they always need to operate with the MPPT operation), which is a tradeoff

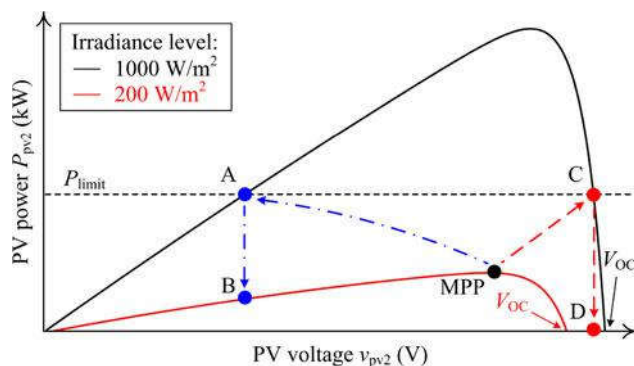


Fig. 6. Possible operating regions of the CPG strategy, where the instability issue during the fast decreasing irradiance condition is illustrated.

between the power reserve capacity and the control accuracy of the DPC strategy.

B. Compensation of the Output Power—CPG Operation for the Slave PV Strings

Once the available power P_{avai} is estimated, the slave PV string has to regulate its output power P_{pv2} in order to provide the total extracted power (from both PV strings) P_{pv} according to (1). As discussed in [10] and [16], the output power of the PV string can be regulated below the MPP using the CPG strategy. From the P-V characteristic of the PV arrays shown in Fig. 6, there are two possible operating points for regulating the PV power P_{pv2} at a certain setpoint P_{limit} (i.e., at A and C in Fig. 6). It has been demonstrated in [16] that the operating region at the right side of the MPP (i.e., at C in Fig. 6) may introduce unstable operation during a fast decreasing irradiance condition (e.g., caused by passing clouds). This is due to the fast decrease in open-circuit voltage of the PV arrays, when the irradiance level suddenly drops (e.g., from 1000 to 200 W/m^2). Under this circumstance, the operating point of the PV system may fall into the open-circuit condition, if the PV system was previously operating at the right side of the MPP (i.e., C \rightarrow D). This is not the case when the PV system regulates the PV power at the left side of the MPP, as the operating point will not go to the open-circuit condition during a fast irradiance drop (i.e., A \rightarrow B). Nevertheless, operating at the lower PV voltage requires a higher conversion ratio (i.e., v_{dc}/v_{pv2}), which it may decrease the efficiency of the boost converter, but it is beyond the scope of this paper [40]. Thus, in order to ensure a stable operation, the PV voltage v_{pv2} is regulated at the left side of the MPP (i.e., at A in Fig. 6) in order to control the PV power according to $P_{pv2} = P_{limit}$.

As discussed previously, one way to reduce the PV power to a certain setpoint is by regulating the PV voltage at the left side of the MPP. This can be achieved by means of the perturb and observe (P&O) CPG algorithm, whose operational principle is illustrated in Fig. 7. Specifically, when the PV power is below the setpoint (i.e., $P_{pv2} \leq P_{limit}$), the MPPT algorithm is employed in order to allow the PV power to reach the setpoint (e.g., shown as the red arrow in Fig. 7). However, once the PV power reaches and starts to exceed the setpoint (i.e., $P_{pv2} > P_{limit}$), the PV

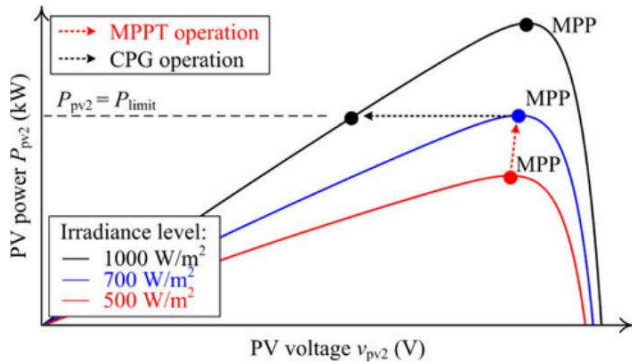


Fig. 7. Operational principle of the CPG scheme based on the P&O-CPG algorithm.

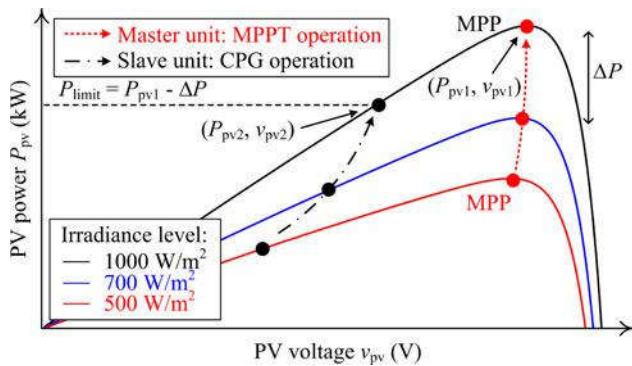


Fig. 8. Operational principle of the DPC with combined MPPT and CPG strategies.

voltage is continuously perturbed toward the left side of the MPP (e.g., by continuously reducing the reference PV voltage) until the PV output power is equal to the setpoint. This is shown as the black arrow in Fig. 7. The reference PV voltage v_{pv2}^* during this operation can be expressed as

$$v_{pv2}^* = v_{MPPT}, \quad \text{when } P_{pv2} \leq P_{limit} \quad (4)$$

$$v_{pv2}^* = v_{MPPT} - v_{step}, \quad \text{when } P_{pv2} > P_{limit}$$

where v_{MPPT} is the reference voltage from the MPPT algorithm (i.e., the P&O MPPT algorithm) and v_{step} is the perturbation step-size of the algorithm.

In contrast to the CPG algorithm in [15]–[17], where a constant setpoint P_{limit} is used, the DPC method dynamically changes the value of the setpoint P_{limit} during the operation in order to achieve the delta power constraint. Since the master PV string is operating in the MPPT mode with the extracted power according to (3), the PV power of the slave PV string P_{pv2} has to be limited according to (8), i.e., $P_{limit} = P_{pv1} - P$

$$P_{pv2} = P_{pv} - P_{pv1} \quad (5)$$

$$= (P_{avail} - P) - P_{pv1} \quad (6)$$

$$= (2P_{pv1} - P) - P_{pv1} \quad (7)$$

$$= P_{pv1} - P. \quad (8)$$

Consequently, the total extracted power according to (1) can be achieved. Fig. 8 illustrates the operational principle of the DPC

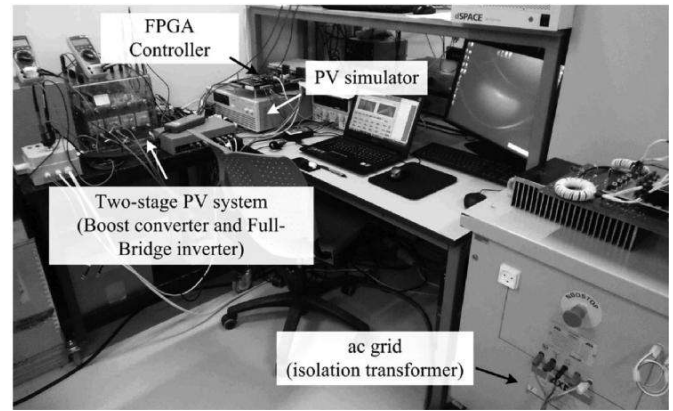


Fig. 9. Experimental setup of the two-stage single-phase grid-connected PV system.

TABLE I
PARAMETERS OF THE TWO-STAGE SINGLE-PHASE GRID-CONNECTED PV SYSTEM (SEE FIG. 4)

PV rated power	3 kW (i.e., 1.5 kW/PV string)
Boost converter inductor	$L = 1.8 \text{ mH}$
PV-side capacitor	$C_{pv} = 1000 \text{ } \mu\text{F}$
LCL -filter	$L_{inv} = 4.8 \text{ mH}, L_g = 2 \text{ mH}, C_f = 4.3 \text{ } \mu\text{F}$
Switching frequency	Boost converter: $f_b = 16 \text{ kHz}$, Full-bridge inverter: $f_{inv} = 8 \text{ kHz}$
DC-link voltage	$V_{dc} = 450 \text{ V}$
Grid nominal voltage (rms)	$V_g = 230 \text{ V}$
Grid nominal frequency	$\omega_0 = 2\pi \times 50 \text{ rad/s}$

strategy where the master PV string is assigned to operate with the MPPT operation and the slave PV string regulates its output power according to (8) by continuously operating in the CPG mode. Notably, P_{pv1} can be easily obtained by measuring i_{pv1} and v_{pv1} (i.e., $P_{pv1} = i_{pv1}v_{pv1}$), as shown in Fig. 5.

IV. PERFORMANCE VERIFICATION OF THE DPC STRATEGY

The effectiveness of the DPC strategy has been verified first on a PLECS/Simulink cosimulation platform and later by experiments with the test rig shown in Fig. 9. In both cases, the system configuration is shown in Fig. 4, where the system parameters are given in Table I. In the tests (both simulations and experiments), the reference power reserve P is chosen to be 200 W, and the DPC strategy is activated when the total PV output power P_{pv} is higher than 2 kW, i.e., $P_{pv} > 2 \text{ kW}$.

First, a trapezoidal solar irradiance profile has been used in simulation, as shown in Fig. 10. It can be seen from the results in Fig. 10(a) that the PV power of the slave PV string P_{pv2} decreases during the DPC operation period by the required amount of power reserve P , compared to P_{pv1} of the master PV string with the MPPT operation. The operational mode transitions can also be observed from the operation P–V trajectory in Fig. 10(b), where P_{pv2} is dynamically regulated at the left side of the MPP (i.e., CPG operation) compared to the MPPT operating trajectory of the master PV string P_{pv1} , when the DPC strategy is activated. Consequently, the total extracted power P_{pv} follows the delta power constraint (i.e.,

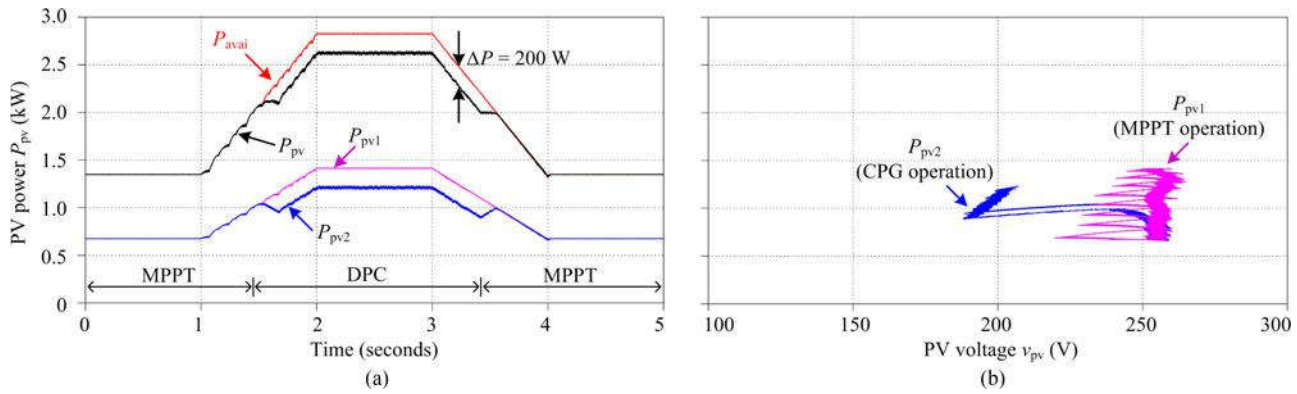


Fig. 10. Simulation results of the DPC strategy under a trapezoidal solar irradiance profile with the reference power reserve P of 200 W: (a) PV output power; and (b) operating trajectory in the P-V curve of the PV panels.

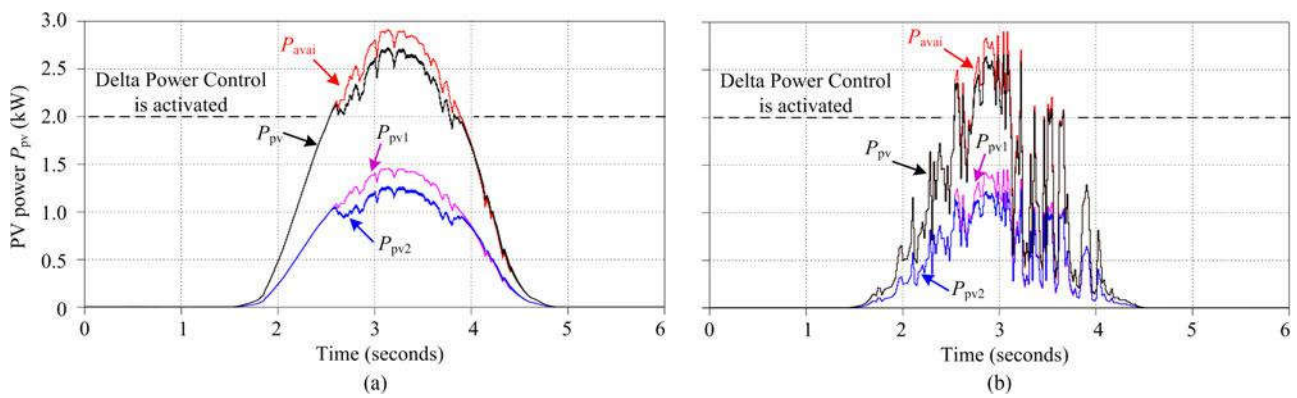


Fig. 11. PV output power (simulations) of the multistring grid-connected PV system with the DPC strategy under: (a) a clear day; and (b) a cloudy day irradiance conditions with the reference power reserve P of 200 W.

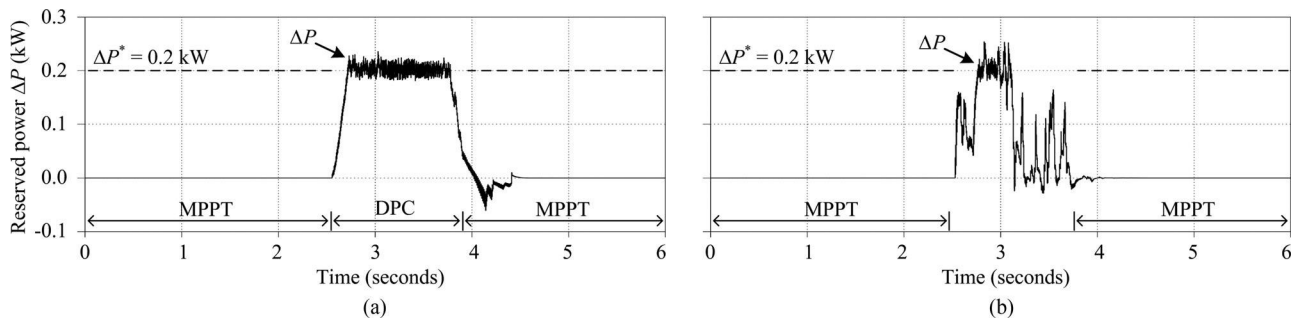


Fig. 12. Reserved power (simulations) of the multistring grid-connected PV system with the DPC strategy under: (a) a clear day; and (b) a cloudy day irradiance conditions with the reference power reserve P of 200 W.

similar to that in Fig. 2). The performances of the DPC strategy are further examined with two real-field daily solar irradiance and temperature profiles through simulations (with accelerated tests due to the limited simulation time). The power extraction of the DPC strategy under a clear day and a cloudy day conditions are shown in Fig. 11. Then, the corresponding re-served power $P = P_{avai} - P_{pv}$ during the operation of the above two conditions is shown in Fig. 12. It can be seen from Figs. 11(a) and 12(a) that the total PV power P_{pv} and the reserved power P are accurately controlled according to the delta power constraint, i.e., $P = 200$ W with the DPC strategy during a clear day condition. Similar behaviors are also observed under

a cloudy day condition in Figs. 11(b) and 12(b). In this case, the dynamics of the controller are more challenged due to the rapidly changing irradiance condition, where the fluctuation in the power reserve is observed. Nevertheless, the reserved power

P can still be controlled with a good accuracy during the DPC operation (e.g., during $t = 2.7-3.2$ s), as shown in Fig. 12(b).

Experimental tests have also been performed with the test rig shown in Fig. 9, in order to verify the effectiveness of the DPC strategy experimentally. In those tests, a PV simulator has been adopted, where the real-field solar irradiance and ambient temperature profiles are programmed in order to emulate the behavior of the PV panels in real operations. It should be

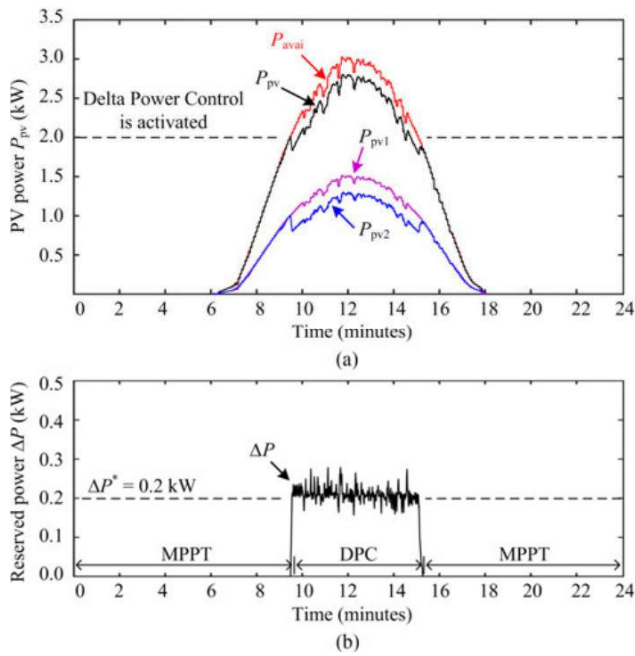


Fig. 13. Experimental results of the multistring grid-connected PV system with DPC strategy under a clear day irradiance condition: (a) PV power; and (b) reserved power with the reference power reserve P of 200 W and the DPC algorithm sampling rate of 10 Hz.

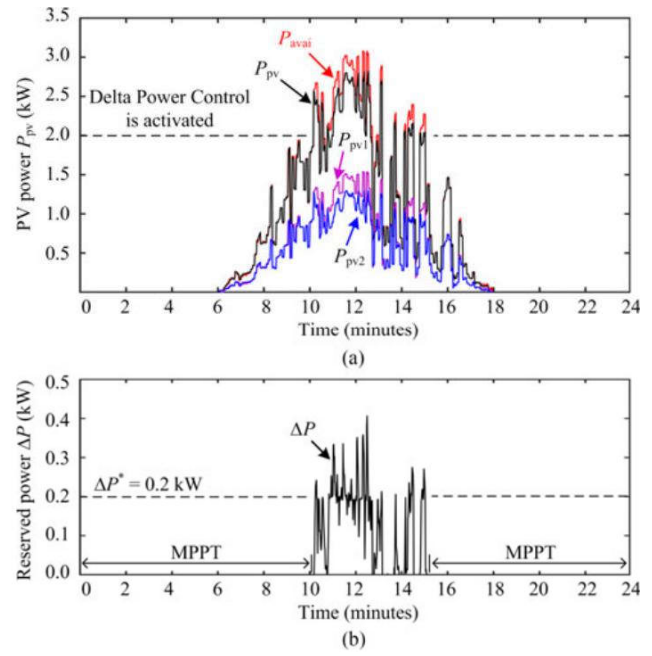


Fig. 15. Experimental results of the multistring grid-connected PV system with DPC strategy under a cloudy day irradiance condition: (a) PV power; and (b) reserved power with the reference power reserve P of 200 W and the DPC algorithm sampling rate of 10 Hz.

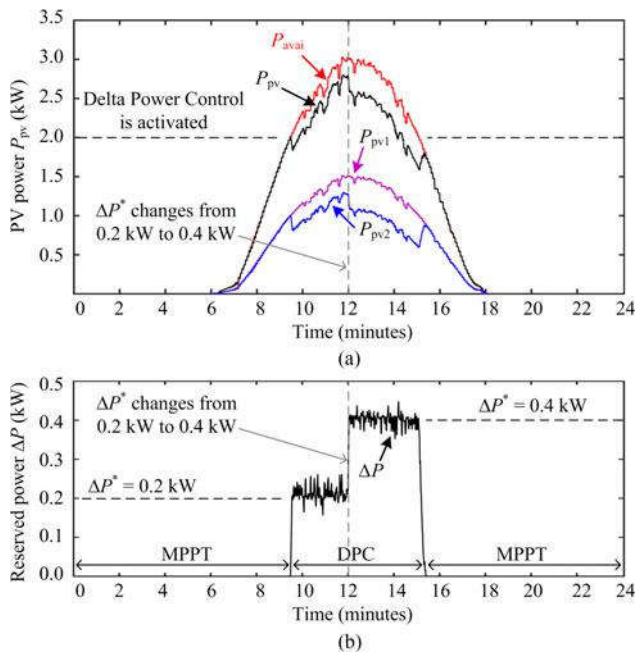


Fig. 14. Experimental results of the multistring grid-connected PV system with DPC strategy under a clear day irradiance condition: (a) PV power; and (b) reserved power with the changing reference power reserve level P from 200 to 400 W and the DPC algorithm sampling rate of 10 Hz.

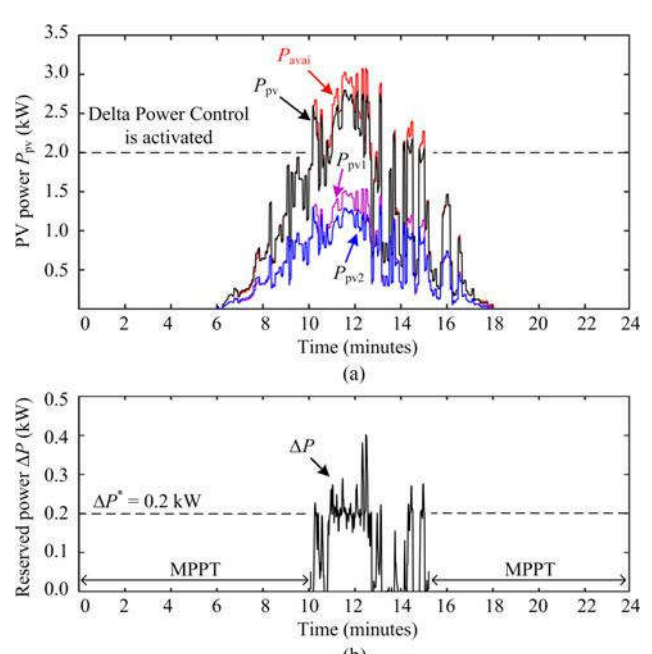


Fig. 16. Experimental results of the multistring grid-connected PV system with DPC strategy under a cloudy day irradiance condition: (a) PV power; and (b) reserved power with the reference power reserve P of 200 W and the DPC algorithm sampling rate of 20 Hz.

mentioned that the coordinated control between the master PV string and the slave PV string is implemented offline due to the availability of lab facilities (only one PV simulator is available). More specifically, the master PV string is first operated with the MPPT operation and its output power P_{pv1} is recorded. Then, the test is repeated for the slave PV string where the recorded

PV output power from the master PV string P_{pv1} is used for as the estimated available power for calculating the setpoint P_{limit} of the CPG strategy for the slave PV string. Also, the accelerated test is adopted in the experiments similar to that in the simulations (i.e., from 24 h to 24 min).

First, the clear day irradiance condition [as shown in Fig. 11(a)] is used, in order to verify the effectiveness of the DPC during slow changing solar irradiance conditions. The PV output power and the corresponding power reserve P are shown in Figs. 13(a) and (b), respectively, where it can be seen that the experimental results are in close agreement with the simulation results shown in Figs. 11(a) and 12(a). The power reserve can be accurately controlled at 200 W during the DPC operation. Further, another test with the changing power reserve condition is carried out in Fig. 14, where a step change in the power reserve reference P from 200 to 400 W is introduced at $t = 12$ min. It can be seen from the results in Fig. 14(a) that the PV power of the slave string P_{pv2} is further reduced when the reference power reserve level increases. As a consequence, the reserved power in Fig. 14(b) can be regulated following the change in the reference value during operation.

The dynamics of the DPC strategy are also examined with a cloudy day irradiance condition, where the control performance of the DPC strategy is highly challenged by a rapid change in the solar irradiance. In this case, the sampling rate of the DPC algorithm (i.e., MPPT and CPG algorithms) becomes important, as it affects the algorithm tracking performance. The experimental results of the DPC strategy with the sampling rate of 10 Hz (which has also been adopted previously in Figs. 13 and 14) are shown in Fig. 15, where a large variation in the power reserve is presented. It can be observed in Fig. 15(b) that the power reserve cannot be maintained at the required value (i.e., 200 W) during a rapid change in the irradiance (e.g., during $t = 10$ –13 min.). This is due to the slow dynamic of the DPC algorithm, which cannot follow the change in the irradiance condition. In order to improve the dynamic performance of the DPC strategy, the sampling rate of DPC strategy is increased to 20 Hz. The experimental results with this case are shown in Fig. 16, where it can be seen from Fig. 16(b) that the variations in the power reserve is reduced, compared to that in Fig. 15(b). Notably, in order to further improve the dynamic performance of the DPC strategy, more advanced MPPT and CPG control strategies with fast dynamics are required, which is a subject for the future work [41]–[43]. Nevertheless, it can be seen that the results carried out via the test rig are in a close agreement with the simulation results. Thus, the experimental results also verify the effectiveness of the DPC strategy.

V. CONCLUSION

A DPC strategy for multistring grid-connected PV systems has been discussed in this paper. In contrast to the prior art solutions, the presented strategy offers a cost-effective solution to the DPC without extra components (e.g., energy storage devices, irradiance measurements). This is achieved by coordinately controlling some PV strings in the master-operation mode (i.e., MPPT) and some in the slave-operation mode (i.e., CPG operation according to the delta power constraint). Particularly, a master PV string operates in the MPPT mode to determine the total available PV power; the other slave PV strings use the estimated available power from the master PV string to calculate their operating point in the P–V characteristic curve of the PV

arrays, and regulate the PV power at the left side of the MPP with the CPG operation. This leads to a delta power production for the entire systems, while ensuring a stable operation. The effectiveness of the DPC strategy has been verified by simulations and experiments, where the delta power production is achieved and the reserved power is accurately controlled.

REFERENCES

- [1] REN21, "Renewables 2016: Global status report (GRS)," 2016. [Online]. Available: <http://www.ren21.net/>
- [2] Solar Power Europe, "Global market outlook for solar power 2016–2020," 2016. [Online]. Available: <http://www.solarpowereurope.org/>
- [3] Fraunhofer ISE, "Recent facts about photovoltaics in Germany," Dec. 2016. [Online]. Available: <http://www.pv-fakten.de/>
- [4] BDEW, "Technical Guideline: Generating Plants Connected to the Medium-Voltage Network, BDEW Bundesverband der Energie- und Wasserwirtschaft e.V.," Berlin, Germany, 2008.
- [5] European Network of Transmission System Operators for Electricity, "Network code for requirements for grid connection applicable to all generators," European Network of Transmission System Operators for Electricity, Brussels, Belgium, Tech. Rep., Mar. 2013. [Online]. Available: <https://www.entsoe.eu.2013>
- [6] Energinet.dk, "Technical regulation 3.2.2 for PV power plants with a power output above 11 kW," Energinet.dk, Fredericia, Denmark, Tech. Rep. no. 14/17997-39, 2015.
- [7] Y. Yang, P. Enjeti, F. Blaabjerg, and H. Wang, "Wide-scale adoption of photovoltaic energy: Grid code modifications are explored in the distribution grid," *IEEE Ind. Appl. Mag.*, vol. 21, no. 5, pp. 21–31, Sep. 2015.
- [8] A. Hoke and D. Maksimovic, "Active power control of photovoltaic power systems," in *Proc. SuSTech*, Aug. 2013, pp. 70–77.
- [9] A. Hoke, E. Muljadi, and D. Maksimovic, "Real-time photovoltaic plant maximum power point estimation for use in grid frequency stabilization," in *16th Workshop Control Model. Power Electron.*, Jul. 2015, pp. 1–7.
- [10] S. Nanou, A. Papakonstantinou, and S. Papanthanasios, "Control of a PV generator to maintain active power reserves during operation," in *Proc. Eur. Photovolt. Solar Energy Conf. Exhib.*, 2012, pp. 4059–4063.
- [11] B.-I. Craciun, T. Kerekes, D. Sera, and R. Teodorescu, "Frequency support functions in large PV power plants with active power reserves," *IEEE J. Emerg. Sel. Topics Power Electron.*, vol. 2, no. 4, pp. 849–858, Dec. 2014.
- [12] National Renewable Energy Laboratory, "On the path to sunshot: The role of advancements in solar photovoltaic efficiency, reliability, and costs," National Renewable Energy Laboratory, Golden, CO, USA, Tech. Rep. No. NREL/TP-6A20-65872, 2016.
- [13] W. A. Omran, M. Kazerani, and M. M. A. Salama, "Investigation of methods for reduction of power fluctuations generated from large grid-connected photovoltaic systems," *IEEE Trans. Energy Convers.*, vol. 26, no. 1, pp. 318–327, Mar. 2011.
- [14] S. Shivashankar, S. Mekhilef, H. Mokhlis, and M. Karimi, "Mitigating methods of power fluctuation of photovoltaic (PV) sources—A review," *Renew. Sustain. Energy Rev.*, vol. 59, pp. 1170–1184, 2016.
- [15] Y. Yang, H. Wang, F. Blaabjerg, and T. Kerekes, "A hybrid power control concept for PV inverters with reduced thermal loading," *IEEE Trans. Power Electron.*, vol. 29, no. 12, pp. 6271–6275, Dec. 2014.
- [16] A. Sangwongwanich, Y. Yang, F. Blaabjerg, and H. Wang, "Benchmarking of constant power generation strategies for single-phase grid-connected photovoltaic systems," in *Proc. IEEE Appl. Power Electron. Conf. Expo.*, Mar. 2016, pp. 370–377.
- [17] A. Sangwongwanich, Y. Yang, and F. Blaabjerg, "High-performance constant power generation in grid-connected PV systems," *IEEE Trans. Power Electron.*, vol. 31, no. 3, pp. 1822–1825, Mar. 2016.
- [18] R. G. Wandhare and V. Agarwal, "Precise active and reactive power control of the PV-DGS integrated with weak grid to increase PV penetration," in *Proc. 40th Photovolt. Spec. Conf.*, Jun. 2014, pp. 3150–3155.
- [19] W. Cao et al., "Two-stage PV inverter system emulator in converter based power grid emulation system," in *Proc. IEEE Energy Convers. Congr. Expo.*, Sep. 2013, pp. 4518–4525.
- [20] C. Rosa, D. Vinikov, E. Romero-Cadaval, V. Pires, and J. Martins, "Low-power home PV systems with MPPT and PC control modes," in *Proc. Int. Conf.-Workshop Compat. Power Electron.*, Jun. 2013, pp. 58–62.
- [21] A. Urtasun, P. Sanchis, and L. Marroyo, "Limiting the power generated by a photovoltaic system," in *Proc. 10th Int. Multi-Conf. Syst., Signals Devices*, Mar. 2013, pp. 1–6.

- [22] L. D. Watson and J. W. Kimball, "Frequency regulation of a microgrid using solar power," in *Proc. IEEE Appl. Power Electron. Conf. Expo.*, Mar. 2011, pp. 321–326.
- [23] S. Bacha, D. Picault, B. Burger, I. Etxeberria-Otadui, and J. Martins, "Photovoltaics in microgrids: An overview of grid integration and energy management aspects," *IEEE Ind. Electron. Mag.*, vol. 9, no. 1, pp. 33–46, Mar. 2015.
- [24] D. Wu, F. Tang, T. Dragicevic, J. C. Vasquez, and J. M. Guerrero, "Autonomous active power control for islanded ac microgrids with photovoltaic generation and energy storage system," *IEEE Trans. Energy*